

# UC Riverside

## UC Riverside Previously Published Works

### Title

Preferential Charge Generation at Aggregate Sites in Narrow Band Gap Infrared Photoresponsive Polymer Semiconductors

### Permalink

<https://escholarship.org/uc/item/4w3000kt>

### Journal

Advanced Optical Materials, 6(7)

### ISSN

2195-1071

### Authors

Sulas, Dana B  
London, Alexander E  
Huang, Lifeng  
[et al.](#)

### Publication Date

2018-04-01

### DOI

10.1002/adom.201701138

Peer reviewed

# Preferential Charge Generation at Aggregate Sites in Narrow Band Gap Infrared Photoresponsive Polymer Semiconductors

Dana B. Sulas, Alexander E. London, Lifeng Huang, Lihua Xu, Zhenghui Wu, Tse Nga Ng, Bryan M. Wong, Cody W. Schlenker, Jason D. Azoulay,\* and Matthew Y. Sfeir\*

Infrared organic photodetector materials are investigated using transient absorption spectroscopy, demonstrating that ultrafast charge generation assisted by polymer aggregation is essential to compensate for the energy gap law, which dictates that excited state lifetimes decrease as the band gap narrows. Short sub-picosecond singlet exciton lifetimes are measured in a structurally related series of infrared-absorbing copolymers that consist of alternating cyclopentadithiophene electron-rich “push” units and strong electron-deficient “pull” units, including benzothiadiazole, benzoselenadiazole, pyridalselenadiazole, or thiadiazoloquinoxaline. While the ultrafast lifetimes of excitons localized on individual polymer chains suggest that charge carrier generation will be inefficient, high detectivity for polymer:PC<sub>71</sub>BM infrared photodetectors is measured in the  $0.6 < \lambda < 1.5 \mu\text{m}$  range. The photophysical processes leading to charge generation are investigated by performing a global analysis on transient absorption data of blended polymer:PC<sub>71</sub>BM films. In these blends, charge carriers form primarily at polymer aggregate sites on the ultrafast time scale (within our instrument response), leaving quickly decaying single-chain excitons unquenched. The results have important implications for the further development of organic infrared optoelectronic devices, where targeting processes such as excited state delocalization over aggregates may be necessary to mitigate losses to ultrafast exciton decay as materials with even lower band gaps are developed.

optoelectronic devices in particular are an appealing alternative to current inorganic technologies, which suffer from limited modularity, intrinsic fragility, low speed, high power consumption, cryogenic cooling requirements, and epitaxial incompatibility with Si complementary metal-oxide-semiconductor (CMOS) processes.<sup>[12]</sup> The beneficial electronic properties of narrow gap OSCs, such as low exciton binding energies and facile charge extraction, stem from their strong intramolecular polarity and easily accessible carrier transport energy levels.<sup>[4,13,14]</sup> However, the strong intramolecular polarity also leads to dramatic and unexpected changes in photophysics, such as ultrafast exciton self-ionization,<sup>[13,14]</sup> emergence of low-energy dark states,<sup>[15]</sup> and singlet fission mediated by intramolecular charge-transfer character.<sup>[16,17]</sup> Rationally designing devices to employ these materials requires a deeper understanding of their unique photophysical properties.

There is a nascent interest in polymeric materials with electronic absorption in the short-wave infrared (SWIR), where recent advances in synthetic techniques have pushed band gaps of solution-processable materials as low as  $\approx 0.5 \text{ eV}$ .<sup>[18–22]</sup> Although further development of structure-function relationships is required to reach even lower band gaps, thus far the successful engineering of narrow gap polymers has, in large part, followed a “push–pull” design strategy in which the energetic difference between the highest occupied molecular orbital (HOMO) and lowest unoccupied molecular orbital (LUMO) is controlled by varying the electron


## 1. Introduction

Organic semiconductors (OSCs) with narrow band gaps and infrared absorption are technologically relevant for a wide range of applications, including harvesting low-energy photons in photovoltaics,<sup>[1–4]</sup> wide bandwidth infrared photodetectors,<sup>[4–8]</sup> and ambipolar field-effect transistors.<sup>[9–11]</sup> Organic infrared

materials as low as  $\approx 0.5 \text{ eV}$ .<sup>[18–22]</sup> Although further development of structure-function relationships is required to reach even lower band gaps, thus far the successful engineering of narrow gap polymers has, in large part, followed a “push–pull” design strategy in which the energetic difference between the highest occupied molecular orbital (HOMO) and lowest unoccupied molecular orbital (LUMO) is controlled by varying the electron

Dr. D. B. Sulas, Prof. C. W. Schlenker  
Department of Chemistry  
University of Washington  
Seattle, WA 98195, USA

A. E. London, L. Huang, Prof. J. D. Azoulay  
School of Polymer Science and Engineering  
The University of Southern Mississippi  
Hattiesburg, MS 39406, USA  
E-mail: jason.azoulay@usm.edu

 The ORCID identification number(s) for the author(s) of this article can be found under <https://doi.org/10.1002/adom.201701138>.

DOI: 10.1002/adom.201701138

L. Xu, Prof. B. M. Wong  
Department of Chemical and Environmental Engineering  
Materials Science and Engineering Program  
University of California, Riverside  
Riverside, CA 92521, USA

Z. Wu, Prof. T. N. Ng  
Department of Electrical and Computer Engineering  
University of California San Diego  
La Jolla, CA 92093, USA

Dr. M. Y. Sfeir  
Center for Functional Nanomaterials  
Brookhaven National Laboratory  
Upton, NY 11794, USA  
E-mail: msfeir@bnl.gov

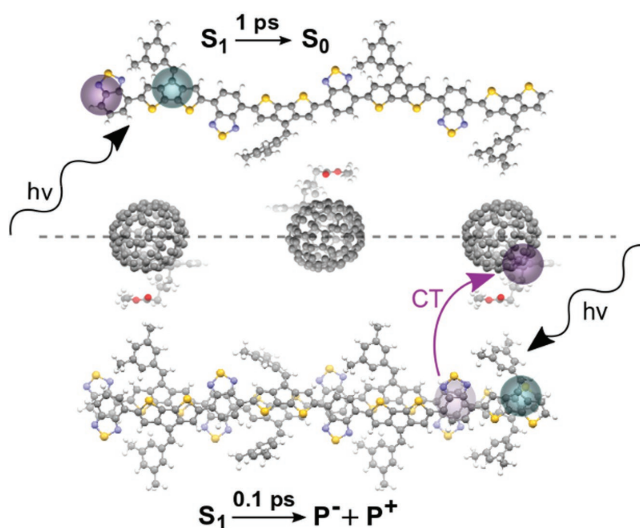
affinity of alternating electron-rich and electron-deficient comonomer units along the polymer backbone.<sup>[7,23–26]</sup> As an alternative strategy to chemical control of the molecular orbital energies, band gaps have been further extended into the infrared through morphological control, creating low-energy aggregate and crystallite states.<sup>[27–30]</sup> This approach is appealing because the optical gap can then be fine-tuned with solution processing,<sup>[27–30]</sup> and because ordered molecular packing often improves the efficiency of charge generation, transport, and extraction.<sup>[30–32]</sup>

Still, the difficult problem of charge photogeneration in standard OSCs becomes even more challenging for infrared absorbers due to additional electronic constraints.<sup>[33,34]</sup> For example, materials with increasingly narrow band gaps face an inherent challenge of decreasing exciton lifetimes, as predicted by the energy gap law.<sup>[15,35–38]</sup> Following the energy gap law, faster nonradiative exciton decay with the narrowing of the band gap is linked to exponentially increasing vibronic wave function overlap (i.e. Franck–Condon factor,  $f_v = \langle \Psi_f | \Psi_i \rangle^2$ ) with decreasing energy between noncrossing potential energy surfaces ( $f_v \sim e^{-\gamma \Delta E}$ , where  $\gamma$  is a constant dependent on molecular parameters that vary between materials).<sup>[38]</sup> While initially introduced in the 1960s for small aromatic molecules,<sup>[39,40]</sup> the energy gap law has been more recently applied to describe the rates of nonradiative decay for both singlet and triplet excitonic states in conjugated OSCs.<sup>[37,41]</sup> Within the traditional picture of optical-to-electrical energy conversion in OSCs, the fast exciton relaxation expected for narrow gap materials could limit the diffusion of bound electron-hole pairs to the donor/acceptor interfaces that drive charge separation, thus limiting extractable photocurrent.<sup>[37,42]</sup>

However, recent reports of charge generation on time scales much faster than predicted by the typical exciton diffusion mechanism prompt the question of whether short exciton lifetimes would pose a limit on efficient charge generation at all.<sup>[14,43–50]</sup> Identifying and harnessing the conditions that lead to carrier generation on sub-100 femtosecond time scales is increasingly important to compensate for the progressively faster exciton decay in narrow gap OSCs. The photophysics leading to ultrafast carrier generation is likely dictated by a mix of energetic and spatial influences. For example, proposed pathways include direct hot carrier excitation and efficient exciton dissociation aided by delocalization of excited states over multiple chromophores.<sup>[45–49,51,52]</sup> Indeed, molecular aggregates and crystalline regions are known to strongly influence device efficiency as well as the dynamics of photoexcited states.<sup>[45,46]</sup>

With an expanding set of novel narrow gap OSCs, it is important to establish structure-function relationships that give rise to their emergent electronic properties. For instance, it is informative to correlate native molecular energetics and relaxation dynamics with systematic chemical modification of the conjugated backbone. Additionally, it is imperative to characterize the extent to which processes in the solid-state such as excited state delocalization over aggregates or donor/acceptor charge transfer could kinetically compete with intramolecular exciton relaxation. To address these issues, we use transient absorption spectroscopy to examine the photophysical pathways for charge generation in systems employing a series of structurally related

### Single chains: ultrafast excited state relaxation



### Aggregates: ultrafast charge generation

**Scheme 1.** Photophysical processes following excitation of electron (purple)–hole (teal) pairs by absorption of light energy ( $h\nu$ ). Single polymer chains (top) exhibit ultrafast ( $\approx 1$  ps) relaxation to the ground state ( $S_0$ ) from singlet excitons ( $S_1$ ), even in blended films with PC<sub>71</sub>BM acceptor molecules. Aggregates (bottom) show extended lifetimes in neat films and exhibit ultrafast polaron formation ( $P^{+/-}$ ,  $\approx 0.1$  ps) in blended films via charge transfer with PC<sub>71</sub>BM.

push–pull semiconducting polymers with progressively narrow band gaps ( $1.14 > E_g^{\text{opt}} > 0.89$  eV) and infrared photoresponse. Although these materials make efficient infrared photodetectors in the  $0.6 < \lambda < 1.5$   $\mu\text{m}$  range,<sup>[7]</sup> we observe short native exciton lifetimes in solution, where sub-picosecond exciton relaxation could conceivably compete with charge transfer in devices. In polymer/fullerene bulk heterojunction films, our global analysis suggests that charge generation on the femtosecond time scale proceeds through aggregate states, while a significant portion of single-chain excitons with sub-picosecond lifetimes remains unquenched (**Scheme 1**). Our analysis provides an important example showing that controlled polymer aggregation is critical for overcoming the inherently short exciton lifetimes in narrow gap OSCs.

## 2. Results and Discussion

We study the process of charge generation in narrow gap OSCs using the series of structurally related polymers shown in **Figure 1**. The polymers consist of alternating electron-rich and electron-deficient groups, where the exocyclic olefin substituted ( $C=CPh$ ) cyclopentadithiophene “push” unit is held constant throughout the copolymer series and the electron-deficient “pull” unit is either 2,1,3-benzothiadiazole (**P1**), a selenium-substituted analog of **P1** containing 2,1,3-benzoselenadiazole (**P2**), a nitrogen-substituted analog of **P2** containing pyridal[2,1,3]selenadiazole (**P3**), or a thiophene-flanked [1,2,5]thiadiazolo[3,4-g]quinoxaline (**P4**). We report the synthesis and physical properties of these polymers in ref. [7]. In addition

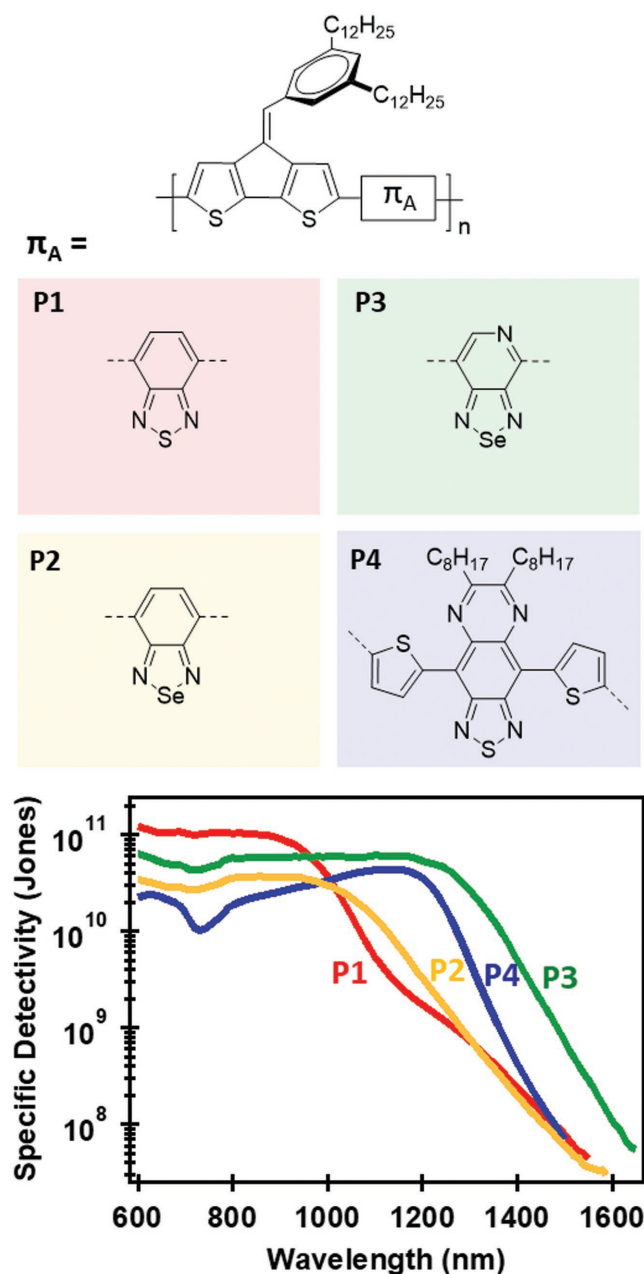


**Figure 1.** Molecular structures of the push–pull polymers used in this study, where all polymers contain an exocyclic olefin substituted cyclopentadithiophene “push” unit, and the “pull” unit ( $\pi_A$ ) varies as 2,1,3-benzothiadiazole for **P1** (red), 2,1,3-benzoselenadiazole for **P2** (yellow), pyridal[2,1,3]selenadiazole for **P3** (green), and thiophene-flanked [1,2,5]thiadiazolo[3,4-g]quinoxaline for **P4** (blue). Lower panel shows the specific detectivities of 1:2 polymer:PC<sub>71</sub>BM photodetectors. Detectivities for **P2–P4** are reproduced with permission.<sup>[7]</sup> Copyright 2017, Royal Society of Chemistry.

to chemical control of HOMO and LUMO energies in this series, lower-energy band gaps are achieved by planarization of the cyclopentadithiophene core and strategic positioning of solubilizing substituents, which mitigate backbone torsion, increase resilience toward conjugation saturation behavior, and enhance intermolecular  $\pi$ – $\pi$  interactions.<sup>[7,53]</sup>

We fabricate SWIR photodetectors by blending the polymers with PC<sub>71</sub>BM, and we measure substantial photocurrent generation in the visible and SWIR. We present the specific detectivities in Figure 1, where the detectivity is proportional to the responsivity of the photodiode divided by the noise current (see Section S5 in the Supporting Information). Interestingly, we note that the NIR photocurrent response extends to energies even lower than the optical gaps of the neat polymers (Figure 2). We attribute the low-energy detectivity partially to polymer aggregate absorption in addition to direct excitation of polymer/PC<sub>71</sub>BM charge-transfer states.<sup>[8]</sup>

We investigate the photophysical processes leading to photocurrent generation by evaluating the effects of chemical modifications in the **P1–P4** series on the band gap energy, the native polymer exciton relaxation kinetics, and the charge generation dynamics in bulk heterojunction films. We note that the polymer structures from **P1** to **P3** only differ by one atom on the acceptor unit. Figure 2a–c show that the closely related **P1–P3** polymers exhibit a trend of red-shifted absorption and decreasing band gap, which is caused by progressive lowering of the LUMO energy as the electron affinity of the acceptor unit increases.<sup>[7,23–25]</sup> In dilute, filtered chlorobenzene solutions, **P1** shows an absorption maximum of 760 nm and an absorption onset of 1.21 eV (Figure 2a), with a shift to 870 nm and 1.08 eV for **P2** (Figure 2b). **P3** (Figure 2c) exhibits a similar absorption maximum as **P2** at 880 nm, but has a significantly broader absorption peak and a lower-energy onset at 0.97 eV.

The polymer **P4** contains the strongest acceptor unit and the lowest energy absorption maxima, with peaks in the solution phase at 960 and 1050 nm and an absorption onset of 0.98 eV (Figure 2d). The molecular structure of **P4** differs significantly from **P1–P3** and incorporates flanking thiophene units into the polymer backbone. For this reason, the lower optical gap of **P4** is attributable to a higher HOMO energy rather than following the trend of decreasing LUMO energy.<sup>[7]</sup> Including **P4** in our study allows us to evaluate the extent to which the trends we observe (such as exciton lifetimes and aggregate-based charge formation) are specific to closely related molecular structures or general across narrow gap OSCs. Using time-dependent density function theory (TD-DFT) calculations, we find similar systematic shifts in absorption to lower energies for the **P1–P4** series (see the Section S6 in the Supporting Information).

Importantly, all narrow gap OSCs in this study show aggregation in thin films, evidenced in Figure 2 by additional low-energy absorption features and aggregate emission spectra. We attribute the red-shifted absorption shoulder to aggregate excitation<sup>[27–29]</sup> and we attribute the filtered solution-phase spectra to absorbing states localized on isolated polymer chains. We note that we characterize the single-chain absorption spectra and kinetics after filtering the solutions to remove aggregates, as these polymers tend to aggregate even in the solution phase. Indeed, the red-shifted absorption peak characteristic of aggregation is present for both the thin films and unfiltered solutions (Figure S2, Supporting Information). Figure S2 (Supporting Information) shows that the aggregate absorption decreases substantially upon filtering. We confirm that the red-shifted absorption denotes aggregation by observing a

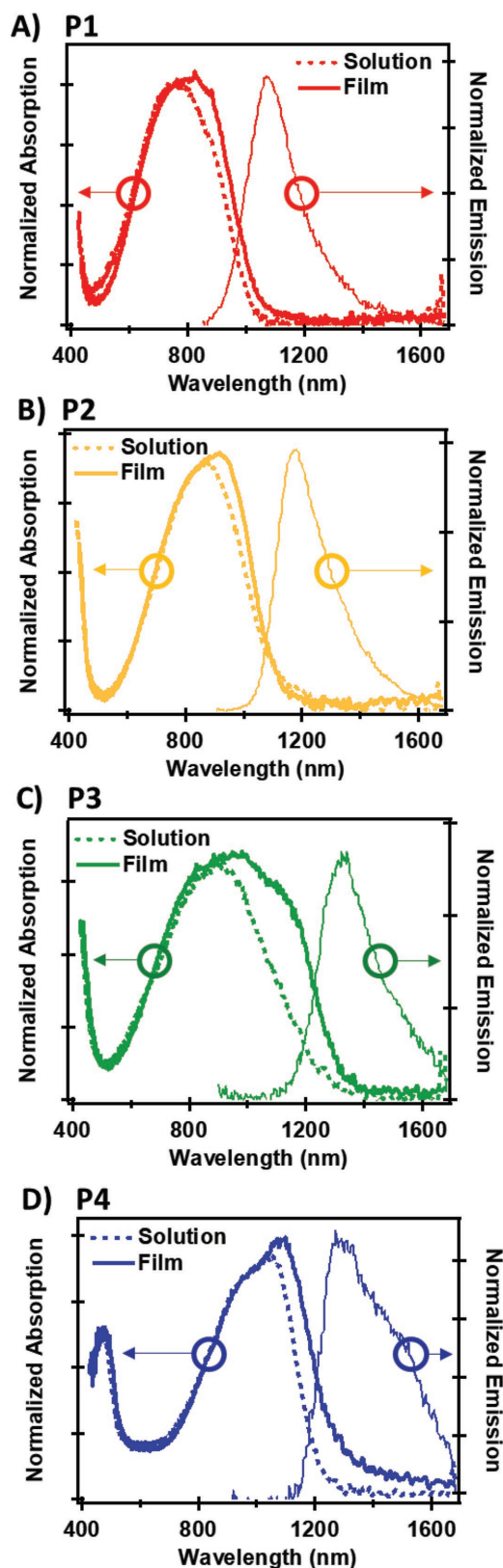


**Figure 2.** Absorption and emission spectra for thin films (solid lines), along with absorption spectra for dilute chlorobenzene solutions (dotted lines) of a) P1, b) P2, c) P3, and d) P4, highlighting additional low-energy absorption peaks in thin films due to polymer aggregation.

decrease in the red-shifted absorption shoulder upon heating the unfiltered solutions to dissolve the aggregates (Figure S1, Supporting Information).

The thin films exhibit aggregate absorption peaks at 850 nm (absorption onset of 1.14 eV) for P1, 930 nm (1.08 eV) for P2, 1150 nm (0.93 eV) for P3, and 1100 nm (0.89 eV) for P4. In addition, we measure aggregate emission peaks at 1070 nm for P1, 1180 nm for P2, 1330 nm for P3, and 1310 nm with a shoulder at 1490 nm for P4. We attribute the emission to aggregate singlet states in the thin films. The emission spectra from single-chain polymers in solution were not measurable under our experimental conditions, likely due to fast nonradiative exciton decay and the tendency for these polymers to aggregate at higher concentrations. From the intersection of the thin-film absorption and emission spectra, we report the  $E_{00}$  aggregate singlet energies as 1.27 eV for P1, 1.15 eV for P2, 1.00 eV for P3, and 1.02 eV for P4. As we will show, polymer aggregation affects the photophysical dynamics in addition to the linear optical properties.

We evaluate the effects of decreasing band gap by measuring the single-chain exciton dynamics in dilute, filtered P1–P4 solutions ( $10^{-5}$  M in repeat units, with  $\approx 10$ –25 repeat units per chain). Figure 3a shows the normalized transient absorption spectra at time zero (co-incident pump and probe), which are characterized by a negative signal (photoinduced transparency) at higher photon energies and a positive signal (photoinduced absorption) extending to lower photon energies. We assign the negative signal to ground-state bleaching due to the spectral coincidence with the linear absorption signal in Figure 2. Consistent with Figure 2, we observe a trend of red-shifting transient absorption bleach minima from P1 to P4. We assign the near infrared photoinduced absorption signal to excited state transitions of single-chain polymer singlet excitons formed immediately upon photoexcitation. These spectral shapes and the associated kinetics for P1–P4 solutions are independent of pump fluence (Figures S4–S11, Supporting Information).

The kinetics of exciton relaxation in dilute P1–P4 polymer solutions is dominated by an ultrafast sub-picosecond decay component (Figure 3b). We monitor the excited state populations for the P1–P4 solutions by fitting the ground-state bleach recovery at the minima. In all four polymers, a  $\approx 0.1$ –0.3 ps component represents more than 60% of the initial amplitude, with 1 or 2 weaker additional components that extend to tens or hundreds of picoseconds. Using global target analysis,<sup>[54]</sup> we show that the weaker components correspond to different transient spectra (Figure S12, Supporting information), implying an evolution in the nature of the excitation. We attribute the spectral evolution to conversion processes such as autoionization in addition to a small contribution from undissolved aggregates (see discussion in the Section S2 in the Supporting Information). We calculate the average single-chain exciton lifetimes using only the components that exhibit the characteristic exciton spectra and determine the averages to be 0.6 ps for P1, 0.4 ps for P2, 0.2 ps for P3, and 1.0 ps for P4.

The singlet lifetimes of the infrared absorbing P1–P4 polymers are anomalously short, even when considering that nonradiative relaxation becomes faster as the optical gap shrinks ( $k_{\text{nonrad}} \sim e^{-\gamma\Delta E}$ ).<sup>[35,37]</sup> For example, the P1–P4 singlet lifetimes

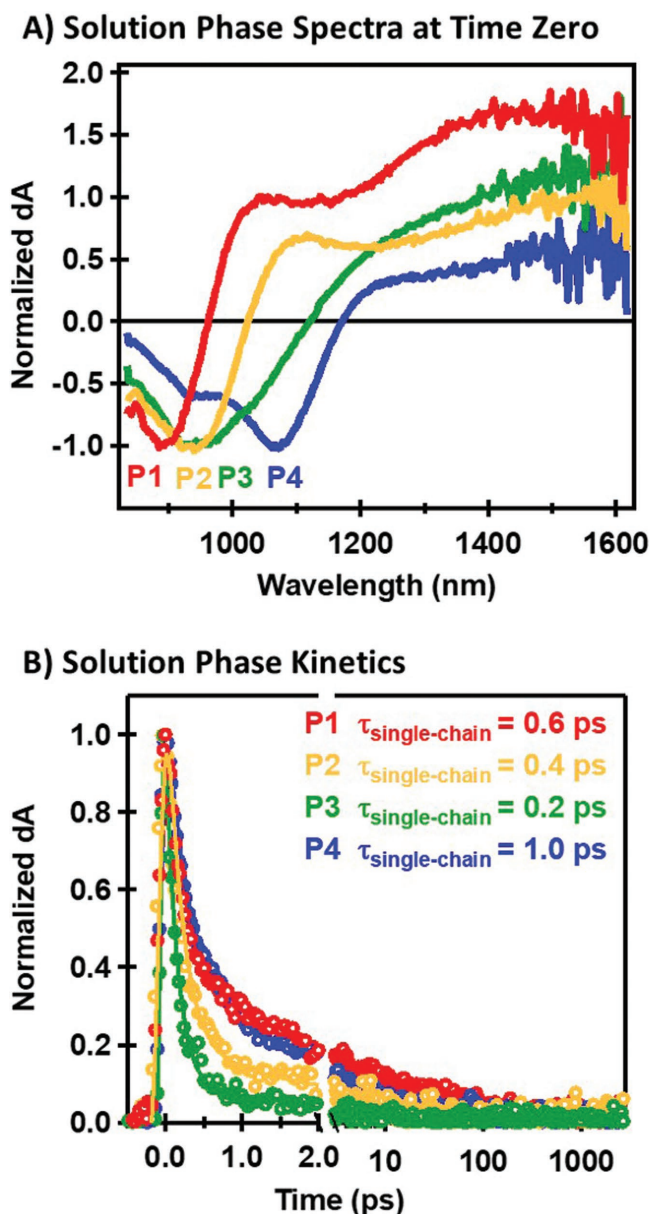


**Figure 3.** a) Transient absorption spectra at time zero along with b) kinetic traces taken at the ground state bleach for chlorobenzene solutions of **P1** (red), **P2** (orange), **P3** (green), and **P4** (blue). Fitted lines overlaying the kinetics data represent multiexponential global fits (see Figure S12 in the Supporting Information). Pump wavelength is 730 nm for **P1–P2**, and 920 nm for **P3–P4**.

are  $\approx 100 \times$  shorter than typical polymers used for photovoltaic applications, including P3HT (470 nm absorption max), PTB7 (680 nm), and PCPDTBT (720 nm) that have singlet lifetimes of 600, 500, and 200 ps, respectively, for isolated chains.<sup>[55,56]</sup> The two orders of magnitude decrease in singlet lifetime is likely a result of the strong intrachain polarity necessary to achieve narrow band gaps and illustrates the challenges of light harvesting with infrared-absorbing polymers. We note that the structurally related **P1–P3** series follows the trend of faster exciton decay with decreasing band gap, as would be predicted by the energy

gap law. However, **P4** shows a slower decay time compared to **P1–P3**, despite having a narrower band gap. In all cases, the single-chain exciton lifetimes are influenced by both the decreasing energy gap as well as the structural differences between polymers. For example, molecular properties such as torsion, symmetry, continuity of the  $\pi$ -electron system, and intermolecular interactions also influence the excited state lifetimes.<sup>[57]</sup> The less pronounced structural differences in the **P1–P3** series are suggestive that the decreasing energy gap could predominately be responsible for the decreasing lifetimes in this case, while the significantly different molecular structure of **P4** could explain the slower decay for **P4**. However, the anomalously short single-chain lifetimes for all polymers in this series indicate that both structure and energetics play critical roles. Deconvoluting these influences would be a fruitful path for further development in this class of materials. Interestingly, our TD-DFT calculations imply that the fast exciton relaxation for all polymers in our study is an intrinsic property of the bright exciton (Section S6, Supporting Information). That is, we find no lower energy dark states at this level of theory that would mediate fast ground state relaxation as occurs in other strong acceptor systems.<sup>[15]</sup>

Compared to the sub-picosecond lifetimes of single-chain excitations, we observe significantly slower exciton relaxation for polymer aggregates in thin films (Figure 4). We observe decay times in thin films over hundreds of picoseconds compared to the 0.2 – 1.0 ps single-chain exciton lifetimes in solution. We provide further analysis of the neat thin-film decays by evaluating the full transient absorption spectra in Section S3 (Supporting Information). In short, the **P1–P3** films exhibit spectral evolution in the first picosecond that we attribute to decay of single-chain excitons, followed by decay on longer time scales of aggregate-based species with red-shifted bleach minima. For **P4** films, we observe only red-shifted aggregate spectra. The presence of both single-chain and aggregate-based excitons following photoexcitation of the **P1–P3** films suggests that both types of excitons may be available for charge transfer with PC<sub>71</sub>BM in these blends, while **P4** blends may be more heavily dominated by aggregate states.

The longer lifetimes and more intense emission that we observe in **P1–P4** polymer films compared to the dilute, filtered solutions indicate longer-lived aggregate singlet states compared to single-chain excitations. The extended lifetimes in thin films are likely due to increased electron–hole separation caused by singlet state delocalization over polymer aggregates.<sup>[58,59]</sup> Indeed, using grazing incidence wide angle X-ray scattering (GIWAXS), we observe ordered  $\pi$ - $\pi$  stacking structure in the neat polymer films (see the Section S7 in the Supporting Information). Significant  $\pi$ - $\pi$  stacking within the aggregates can enable delocalization over neighboring polymer chains, leading to partial donor–donor charge-transfer characteristics among aggregated chains.<sup>[59,60]</sup> These longer-lived dynamics that we observe in the **P1–P4** thin films compared to solutions are consistent with systems exhibiting partial charge-transfer character within the donor phase,<sup>[59,60]</sup> but distinguish these materials from other polymer semiconductor systems in which singlet states decay more quickly in thin films compared to solutions.<sup>[56]</sup> For other systems with faster decay dynamics for aggregate states, relaxation in thin films could be accelerated

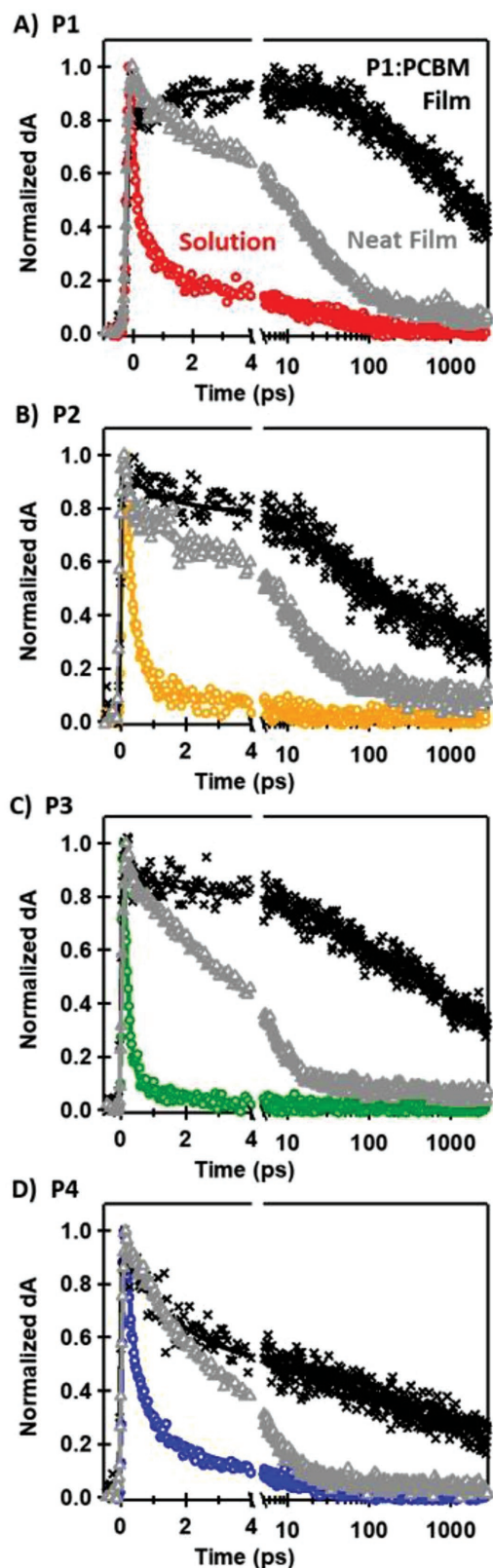


**Figure 4.** Comparison of bleach decay in solutions (colored), neat films (gray), and PCBM blended films (black) for a) P1, b) P2, c) P3, and d) P4. Solution-phase data are taken from Figure 2. Neat film and polymer:PC<sub>71</sub>BM data are collected at  $2\text{--}4 \times 10^{17}$  absorbed photons  $\text{cm}^{-3}$  at pump wavelengths of 620 nm for P1, 730 nm for P2, and 920 nm for P3–P4.

by effects such as increased nonradiative recombination losses with decreasing intermolecular distance<sup>[61]</sup> or exciton diffusion to impurities.<sup>[56]</sup>

In addition to increasing the excited state lifetime, we find that aggregates play a predominant role in facilitating charge transfer at donor/acceptor interfaces with PC<sub>71</sub>BM. Figure 4 shows significantly slower bleach recovery dynamics in 1:2 polymer:PC<sub>71</sub>BM bulk heterojunction films compared to solutions and neat thin films. We attribute the longer-lived kinetics to free carriers formed following charge transfer in the blends, consistent with our extraction of photocurrent from polymer:PC<sub>71</sub>BM devices in Figure 1. Indeed, we find that the long-lived transient absorption spectra in the blends match the polymer cation spectra that we measure following electrochemical oxidation (Figure 6). In addition, the decay kinetics in the blends become faster with increasing pump fluence (Figures S22–S26, Supporting Information), as expected for bimolecular carrier recombination.<sup>[62–64]</sup>

Our observation of significant polymer cation formation in bulk heterojunction films reveals that the short picosecond intrinsic lifetimes of single-chain excitons do not prohibit charge generation. However, we find that charge generation preferentially occurs at aggregate sites, while excitons formed on isolated polymer chains primarily relax to the ground state. We distinguish between cation formation at aggregate or at single-chain sites by considering the evolution of the transient absorption bleach position in the blended films as a function of time. For illustration, Figure 5a,b shows the red shift of the bleach minimum over time in P1:PC<sub>71</sub>BM blended films. The blend spectrum initially resembles a mixture of single-chain and aggregate bleach signals, and at later times resembles the red shifted aggregate bleach position. For comparison, we provide representative bleach spectra for single-chain or aggregate excitations in Figure 5c, given by P1 dilute solutions (890 nm minimum) and neat films (960 nm minimum), respectively.

The initial red shift of the bleach position in the blends suggests a contribution from quickly decaying single-chain excitons, and the continued red shifting suggests that excitations relax to lower energy sites over time, with long-lived charge carriers persisting primarily at aggregate sites.<sup>[46,48,64,65]</sup> We next separate the time-dependent contributions from single-chain and aggregate excitations to carrier formation by performing a global target analysis on the transient absorption spectra for all polymer:PC<sub>71</sub>BM blends (Figure 6).<sup>[54]</sup>

While photoexcitation occurs everywhere within the film, our analysis indicates that carriers form primarily at aggregate sites and single-chain excitations do not materially contribute to charge generation. In Figure 6, we show fitted spectral components that make up the polymer:PC<sub>71</sub>BM transient absorption data, along with their relative concentrations over time. We normalize all spectral components to the bleach minima (Figure 6a–d), and scale the relative concentrations based on the bleach contribution to the total transient absorption spectrum (Figure 6e–h). For P1–P3 blends, one of the spectral components (black circles) exhibits a line shape reminiscent of the single-chain exciton spectrum that we obtain for the dilute polymer solutions in Figure 3. Figure 6e–g shows that this component is formed immediately upon

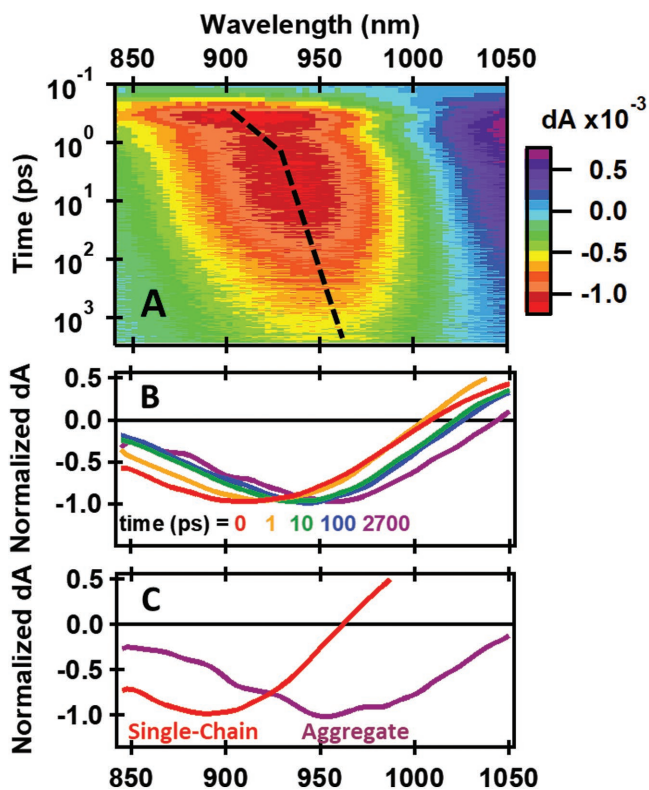


**Figure 5.** a) Contour plot of transient absorption spectra in the bleach region for the **P1**:PC<sub>71</sub>BM blend under 630 nm photoexcitation, showing relaxation of the **P1** bleach to lower energies over time. Black dashed line is a guide for the eye. b) Normalized spectra of the **P1**:PC<sub>71</sub>BM blend at time slices between 0 and 2.7 ns. c) Normalized spectrum of the **P1** solution at time zero, highlighting the bleach position corresponding to single polymer chains, along with the normalized spectrum of neat **P1** films at 2.5 ns, highlighting the bleach position corresponding to polymer aggregates.

photoexcitation and decays with a lifetime of 0.6–2.0 ps. Based on the short lifetime and similarity to solution-phase data, we conclude that single-chain excitons are photoexcited in the **P1**–**P3** bulk heterojunction films but remain largely unquenched.

Rather than dissociation of single-chain excitons, we find that charge generation occurs impulsively at aggregate sites through an ultrafast pathway that does not exploit the longer-lived aggregate excitons. We demonstrate aggregate-based charge generation in the **P1**–**P3** blends by extracting spectral components (red triangles and blue squares in Figure 6a–c) with line shapes similar to the cation spectra for electrochemically oxidized polymer films (gray traces in Figure 6a–c). Both extracted aggregate cation spectra show similar line shapes to each other and red shifted bleach minima compared to the single-chain exciton spectra.

The aggregate cation spectra account for the majority of the transient absorption signal in the **P1**–**P3** blends at early times, with a much weaker contribution from unquenched single-chain excitons. Figure 6e–g shows that the cation component marked by red triangles is formed immediately upon photoexcitation and transforms into the component marked by blue

squares with a 45–115 ps time constant. The blue trace then persists with lifetime >3 ns. The slight red shift between the two cation spectra indicates relaxation to lower energies over time, consistent with Figure 5.

The fast charge generation along with preferential charge formation at aggregates compared to localized single-chain sites may be related to excited state delocalization over the aggregates.<sup>[45–49,51,52]</sup> Indeed, these observations are consistent with a growing body of literature implicating delocalized states in the formation of charge carriers on sub-picosecond time scales.<sup>[45–49,51,52]</sup> Our analysis thus points toward aggregation as a key factor in carrier formation for narrow gap OSCs despite increasingly fast single-chain exciton decay.

The data for the **P4**:PC<sub>71</sub>BM blends show similar charge generation dynamics to the **P1**–**P3** blends with a few notable exceptions. Unlike the fitted spectra for the **P1**–**P3** blends, all three of the spectral components for the **P4**:PC<sub>71</sub>BM films in Figure 6d have similar bleach minima. The absence of a blue-shifted spectral component reminiscent of single-chain excitons in **P4**:PC<sub>71</sub>BM films suggests that **P4** is prone to aggregation and few isolated polymer chains remain in the condensed phase. While charge generation continues to proceed via aggregate states in the **P4** blends, a significant fraction of **P4** aggregate excitons remains unquenched. We attribute the component represented by black circles in Figure 6d to unquenched aggregate excitons, based on the relatively fast decay (1.9 ps in Figure 6h), red shifted bleach, and similarity to the dominant spectral component in the neat film spectra (Figures S13d and S22d, Supporting Information). The unquenched aggregate excitons in the **P4** blends are evidence that **P4** aggregates are large, and excitations originating far from a **P4**/PC<sub>71</sub>BM interface do not efficiently undergo charge generation.

However, similar to the **P1**–**P3** blends, the **P4** blends show ultrafast charge generation, with the aggregate cation spectral component accounting for the majority of the transient absorption signal at early times. The long-lived components that we assign to cations (red triangles and blue squares in Figure 6d) resemble electrochemically oxidized **P4** films (gray trace) and decay with fluence-dependent kinetics (Figure S22h, Supporting Information). The similar aggregate-based ultrafast charge generation in **P4** blends suggests that this pathway is applicable even for narrow gap materials with molecular structures outside of the closely related **P1**–**P3** series.

### 3. Conclusion

Our study implies that optimizing performance from devices employing narrow gap OSCs requires fabrication tactics that target nontraditional mechanisms of charge generation. In particular, we show that polymer aggregation plays a key role in ultrafast carrier formation while avoiding limitations from quickly decaying excitons in these infrared-absorbing materials.

We measure increasingly fast sub-picosecond native exciton decay rates in our structurally related series of narrow gap materials. Although aggregates in thin films exhibit longer exciton lifetimes compared to single polymer chains in solution,



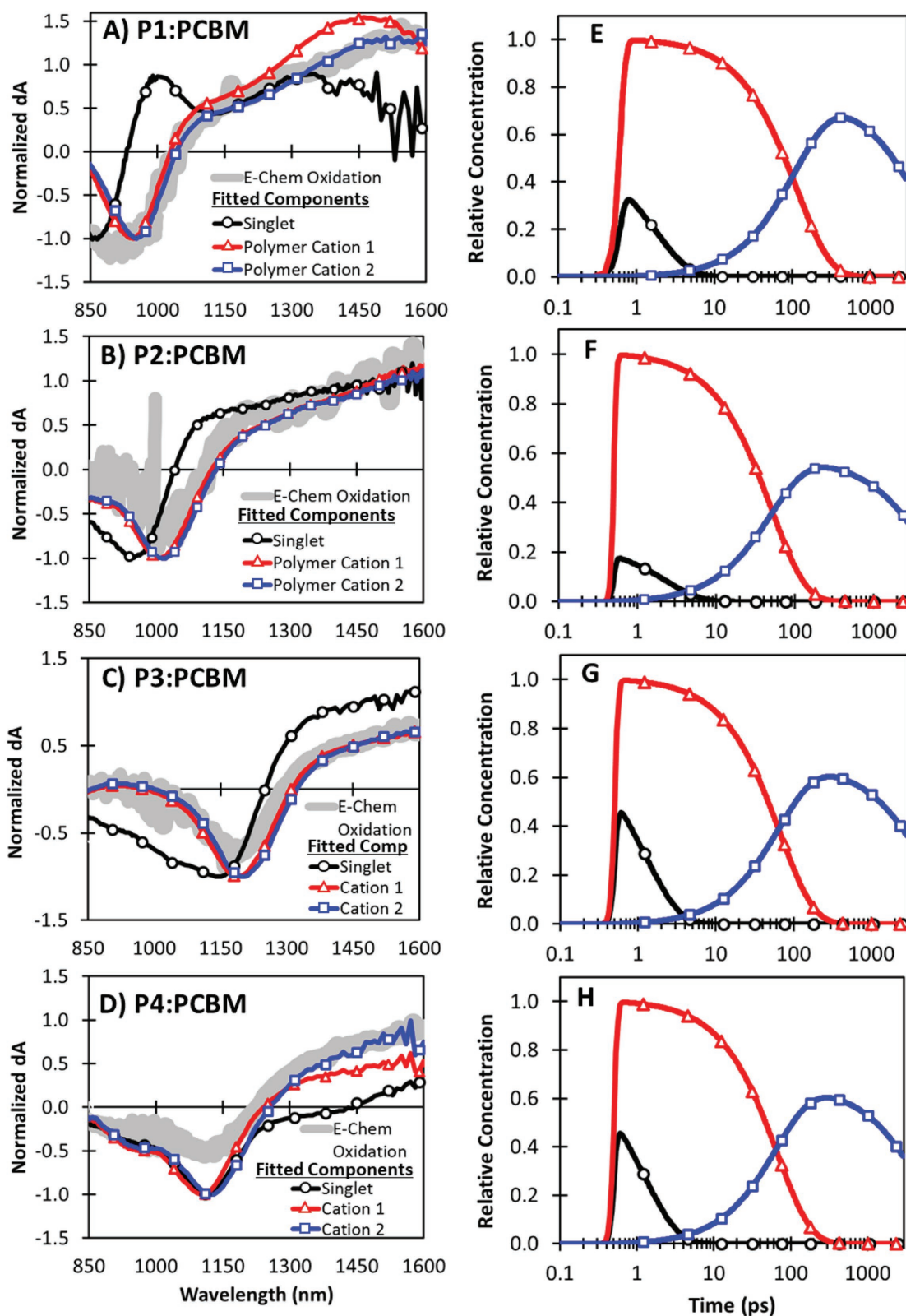


**Figure 6.** Fitted spectral components from global target analysis of transient absorption data for thin films of a) **P1:PC<sub>71</sub>BM**, b) **P2:PC<sub>71</sub>BM**, c) **P3:PC<sub>71</sub>BM**, and d) **P4:PC<sub>71</sub>BM**. Spectral components represent unquenched polymer singlets (black circles) and polymer cations (blue squares and red triangles). Fitted spectra are overlaid with the normalized polymer cation spectra from spectroelectrochemical oxidation of polymer films on indium tin oxide (gray). Corresponding fitted kinetics traces for each spectral component in e) **P1:PC<sub>71</sub>BM**, f) **P2:PC<sub>71</sub>BM**, g) **P3:PC<sub>71</sub>BM**, and h) **P4:PC<sub>71</sub>BM**. Data used for these fits were collected at pump fluence of  $0.3\text{--}0.5 \times 10^{18}$  absorbed photons  $\text{cm}^{-2}$ .

we find that charge generation in blends with PC<sub>71</sub>BM likely bypasses the traditionally assumed process of localized exciton hopping to the donor/acceptor interface. Instead, global target analysis of our transient absorption data suggests that charge carriers form preferentially at aggregate sites on the ultrafast time scale, within our instrument response time. These results present an important example detailing ultrafast pathways for charge generation in molecularly similar narrow gap polymer semiconductors.

## Supporting Information

Supporting Information is available from the Wiley Online Library or from the author.

## Acknowledgements

The authors thank Linda Peteanu for helpful discussion on polymer aggregation, and Song Zhang and Xiaodan Gu for assistance with GIWAXS measurements. D.B.S. was supported by the National Science Foundation Graduate Research Internship Program and the NSF Graduate Research Fellowship Program (2013118402). This research used resources of the Center for Functional Nanomaterials, which is a U.S. DOE Office of Science Facility, at Brookhaven National Laboratory under Contract No. DE-SC0012704. All DFT and TD-DFT calculations by L.X. and B.M.W. were supported by the U.S. Department of Energy, Office of Science, Early Career Research Program under Award No. DE-SC0016269. L.X. also acknowledges a Global Food Initiative Student Fellowship for partial support. A.E.L., L.H., and J.D.A. are grateful for support from the National Science Foundation (NSF OIA-1632825) and the Air Force Office of Scientific Research (AFOSR) through the Organic Materials Chemistry Program (Grant Number: FA9550-17-1-0261, Program Manager: Dr. Kenneth Caster). Z. W. and T. N. N. acknowledge support from the NSF (CMMI-1635729).

## Conflict of Interest

The authors declare no conflict of interest.

## Keywords

bulk heterojunction, delocalization, organic electronics, push–pull, ultrafast spectroscopy

Received: October 23, 2017  
Revised: December 22, 2017  
Published online: February 13, 2018

- [1] L. Bian, J. Miao, J. Hai, E. Zhu, J. Yu, G. Ge, H. Wu, W. Tang, *RSC Adv.* **2014**, *4*, 53939.
- [2] O. V. Kozlov, V. G. Pavelyev, H. D. de Gier, R. W. A. Havenith, P. H. M. van Loosdrecht, J. C. Hummelen, M. S. Pshenichnikov, *Org. Photon. Photovolt.* **2016**, *4*, 24.
- [3] K. H. Hendriks, W. Li, M. M. Wienk, R. A. J. Janssen, *J. Am. Chem. Soc.* **2014**, *136*, 12130.
- [4] L. Dou, Y. Liu, Z. Hong, G. Li, Y. Yang, *Chem. Rev.* **2015**, *115*, 12633.
- [5] X. Gong, M. Tong, Y. Xia, W. Cai, J. S. Moon, Y. Cao, G. Yu, C.-L. Shieh, B. Nilsson, A. J. Heeger, *Science* **2009**, *325*, 1665.
- [6] Z. Wu, W. Yao, A. E. London, J. D. Azoulay, T. N. Ng, *ACS Appl. Mater. Interfaces* **2017**, *9*, 1654.
- [7] A. E. London, L. Huang, B. A. Zhang, M. B. Oviedo, J. Tropp, W. Yao, Z. Wu, B. M. Wong, T. N. Ng, J. D. Azoulay, *Polym. Chem.* **2017**, *8*, 2922.
- [8] B. Siegmund, A. Mischok, J. Benduhn, O. Zeika, S. Ullbrich, F. Nehm, M. Böhm, D. Spoltore, H. Fröb, C. Körner, K. Leo, K. Vandewal, *Nat. Commun.* **2017**, *8*, 15421.
- [9] J. D. Yuen, F. Wudl, *Energy Environ. Sci.* **2013**, *6*, 392.
- [10] Y. Zhao, Y. Guo, Y. Liu, *Adv. Mater.* **2013**, *25*, 5372.
- [11] C. An, M. Li, T. Marszalek, D. Li, R. Berger, W. Pisula, M. Baumgarten, *Chem. Mater.* **2014**, *26*, 5923.
- [12] A. Rogalski, *Infrared Phys. Technol.* **2002**, *43*, 187.
- [13] B. S. Rolczynski, J. M. Szarko, H. J. Son, Y. Liang, L. Yu, L. X. Chen, *J. Am. Chem. Soc.* **2012**, *134*, 4142.
- [14] B. S. Rolczynski, J. M. Szarko, H. J. Son, L. Yu, L. X. Chen, *J. Phys. Chem. Lett.* **2014**, *5*, 1856.
- [15] E. Busby, J. Xia, J. Z. Low, Q. Wu, J. Hoy, L. M. Campos, M. Y. Sfeir, *J. Phys. Chem. B* **2015**, *119*, 7644.
- [16] Y. Kasai, Y. Tamai, H. Ohkita, H. Benten, S. Ito, *J. Am. Chem. Soc.* **2015**, *137*, 15980.
- [17] E. Busby, J. Xia, Q. Wu, J. Z. Low, R. Song, J. R. Miller, X. Y. Zhu, L. M. Campos, M. Y. Sfeir, *Nat. Mater.* **2015**, *14*, 426.
- [18] M. E. Foster, B. A. Zhang, D. Murtagh, Y. Liu, M. Y. Sfeir, B. M. Wong, J. D. Azoulay, *Macromol. Rapid Commun.* **2014**, *35*, 1516.
- [19] T. T. Steckler, P. Henriksson, S. Mollinger, A. Lundin, A. Salleo, M. R. Andersson, *J. Am. Chem. Soc.* **2014**, *136*, 1190.
- [20] J. D. Yuen, M. Wang, J. Fan, D. Sheberla, M. Kemei, N. Banerji, M. Scarongella, S. Valouch, T. Pho, R. Kumar, E. C. Chesnut, M. Bendikov, F. Wudl, *J. Polym. Sci., Part A: Polym. Chem.* **2015**, *53*, 287.
- [21] J. Fan, J. D. Yuen, M. Wang, J. Seifert, J.-H. Seo, A. R. Mohebbi, D. Zakhidov, A. Heeger, F. Wudl, *Adv. Mater.* **2012**, *24*, 2186.
- [22] J. Fan, J. D. Yuen, W. Cui, J. Seifert, A. R. Mohebbi, M. Wang, H. Zhou, A. Heeger, F. Wudl, *Adv. Mater.* **2012**, *24*, 6164.
- [23] S. D. Oosterhout, N. Kopidakis, Z. R. Owczarczyk, W. A. Braunecker, R. E. Larsen, E. L. Ratcliff, D. C. Olson, *J. Mater. Chem. A* **2015**, *3*, 9777.
- [24] G. L. Gibson, T. M. McCormick, D. S. Seferos, *J. Am. Chem. Soc.* **2012**, *134*, 539.
- [25] A. Casey, S. D. Dimitrov, P. Shakya-Tuladhar, Z. Fei, M. Nguyen, Y. Han, T. D. Anthopoulos, J. R. Durrant, M. Heeney, *Chem. Mater.* **2016**, *28*, 5110.
- [26] J. Shao, G. Wang, K. Wang, C. Yang, M. Wang, *Polym. Chem.* **2015**, *6*, 6836.
- [27] S. L. Fronk, M. Wang, M. Ford, J. Coughlin, C.-K. Mai, G. C. Bazan, *Chem. Sci.* **2016**, *7*, 5313.
- [28] C. Scharsich, F. S. U. Fischer, K. Wilma, R. Hildner, S. Ludwigs, A. Köhler, *J. Polym. Sci., Part B: Polym. Phys.* **2015**, *53*, 1416.
- [29] J. Peet, J. Y. Kim, N. E. Coates, W. L. Ma, D. Moses, A. J. Heeger, G. C. Bazan, *Nat. Mater.* **2007**, *6*, 497.
- [30] Y. Liu, J. Zhao, Z. Li, C. Mu, W. Ma, H. Hu, K. Jiang, H. Lin, H. Ade, H. Yan, *Nat. Commun.* **2014**, *5*, 5293.
- [31] C. Kastner, D. A. M. Egbe, H. Hoppe, *J. Mat. Chem. A* **2015**, *3*, 395.
- [32] R. Noriega, J. Rivnay, K. Vandewal, F. P. V. Koch, N. Stingelin, P. Smith, M. F. Toney, A. Salleo, *Nat. Mater.* **2013**, *12*, 1038.
- [33] D. B. Rodovsky, J. Peet, N. Shao, J. D. Azoulay, G. C. Bazan, N. Drolet, Q. Wu, M. Y. Sfeir, *J. Phys. Chem. C* **2013**, *117*, 25955.
- [34] D. C. Coffey, B. W. Larson, A. W. Hains, J. B. Whitaker, N. Kopidakis, O. V. Boltalina, S. H. Strauss, G. Rumbles, *J. Phys. Chem. C* **2012**, *116*, 8916.
- [35] R. Englman, J. Jortner, *Mol. Phys.* **1970**, *18*, 145.
- [36] W. Siebrand, *Chem. Phys. Lett.* **1971**, *9*, 157.
- [37] D. S. Dimitrov, C. B. Schroeder, B. C. Nielsen, H. Bronstein, Z. Fei, I. McCulloch, M. Heeney, R. J. Durrant, *Polymers* **2016**, *8*, 14.

- [38] N. J. Turro, V. Ramamurthy, J. C. Scaiano, *Principles of Molecular Photochemistry*. University Science Books, Sausalita, California 2009.
- [39] W. Siebrand, *J. Chem. Phys.* **1967**, *46*, 440.
- [40] G. W. Robinson, R. P. Frosch, *J. Chem. Phys.* **1963**, *38*, 1187.
- [41] J. S. Wilson, N. Chawdhury, M. R. A. Al-Mandhary, M. Younus, M. S. Khan, P. R. Raithby, A. Köhler, R. H. Friend, *J. Am. Chem. Soc.* **2001**, *123*, 9412.
- [42] Y. Tamai, H. Ohkita, H. Benten, S. Ito, *J. Phys. Chem. Lett.* **2015**, *6*, 3417.
- [43] Z. S. Wang, W. E. I. Sha, W. C. H. Choy, *J. Appl. Phys.* **2016**, *120*, 213101.
- [44] M. Causa, J. De Jonghe-Risse, M. Scarongella, J. C. Brauer, E. Buchaca-Domingo, J. E. Moser, N. Stingelin, N. Banerji, *Nat. Commun.* **2016**, *7*, 12556.
- [45] A. C. Jakowetz, M. L. Böhm, J. Zhang, A. Sadhanala, S. Huettner, A. A. Bakulin, A. Rao, R. H. Friend, *J. Am. Chem. Soc.* **2016**, *138*, 11672.
- [46] A. C. Jakowetz, M. L. Bohm, A. Sadhanala, S. Huettner, A. Rao, R. H. Friend, *Nat. Mater.* **2017**, *16*, 551.
- [47] H. Bassler, A. Kohler, *Phys. Chem. Chem. Phys.* **2015**, *17*, 28451.
- [48] L. G. Kaake, J. J. Jasieniak, R. C. Bakus, G. C. Welch, D. Moses, G. C. Bazan, A. J. Heeger, *J. Am. Chem. Soc.* **2012**, *134*, 19828.
- [49] G. Grancini, M. Maiuri, D. Fazzi, A. Petrozza, H. J. Egelhaaf, D. Brida, G. Cerullo, G. Lanzani, *Nat. Mater.* **2013**, *12*, 29.
- [50] C. Dyer-Smith, I. A. Howard, C. Cabanetos, A. El Labban, P. M. Beaujuge, F. Laquai, *Adv. Energy Mater.* **2015**, *5*, 1401778.
- [51] S. D. Dimitrov, A. A. Bakulin, C. B. Nielsen, B. C. Schroeder, J. Du, H. Bronstein, I. McCulloch, R. H. Friend, J. R. Durrant, *J. Am. Chem. Soc.* **2012**, *134*, 18189.
- [52] A. A. Bakulin, A. Rao, V. G. Pavelyev, P. H. M. van Loosdrecht, M. S. Pshenichnikov, D. Niedzialek, J. Cornil, D. Beljonne, R. H. Friend, *Science* **2012**, *335*, 1340.
- [53] D. Venkateshvaran, M. Nikolka, A. Sadhanala, V. Lemaire, M. Zelazny, M. Kepa, M. Hurhangee, A. J. Kronemeijer, V. Pecunia, I. Nasrallah, I. Romanov, K. Broch, I. McCulloch, D. Emin, Y. Olivier, J. Cornil, D. Beljonne, H. Sirringhaus, *Nature* **2014**, *515*, 384.
- [54] J. J. Snellenburg, S. P. Laptinok, R. Seger, K. M. Mullen, I. H. M. van Stokkum, *J. Stat. Softw.* **2012**, *49*, 1.
- [55] S. Cho, B. S. Rolczynski, T. Xu, L. Yu, L. X. Chen, *J. Phys. Chem. B* **2015**, *119*, 7447.
- [56] O. V. Mikhnenko, M. Kuik, J. Lin, N. van der Kaap, T.-Q. Nguyen, P. W. M. Blom, *Adv. Mater.* **2014**, *26*, 1912.
- [57] A. Thiessen, D. Würsch, S.-S. Jester, A. V. Aggarwal, A. Idelson, S. Bange, J. Vogelsang, S. Höger, J. M. Lupton, *J. Phys. Chem. B* **2015**, *119*, 9949.
- [58] B. W. Caplins, T. K. Mullenbach, R. J. Holmes, D. A. Blank, *J. Phys. Chem. C* **2015**, *119*, 27340.
- [59] T. Stangl, P. Wilhelm, K. Remmerssen, S. Höger, J. Vogelsang, J. M. Lupton, *Proc. Natl. Acad. Sci. USA* **2015**, *112*, E5560.
- [60] O. G. Reid, R. D. Pensack, Y. Song, G. D. Scholes, G. Rumbles, *Chem. Mater.* **2014**, *26*, 561.
- [61] S. M. Menke, W. A. Luhman, R. J. Holmes, *Nat. Mater.* **2013**, *12*, 152.
- [62] P. C. Y. Chow, S. Gelinas, A. Rao, R. H. Friend, *J. Am. Chem. Soc.* **2014**, *136*, 3424.
- [63] G. Lakhwani, A. Rao, R. H. Friend, *Annu. Rev. Phys. Chem.* **2014**, *65*, 557.
- [64] F. Etzold, I. A. Howard, R. Mauer, M. Meister, T.-D. Kim, K.-S. Lee, N. S. Baek, F. Laquai, *J. Am. Chem. Soc.* **2011**, *133*, 9469.
- [65] I. A. Howard, F. Etzold, F. Laquai, M. Kemerink, *Adv. Energy Mater.* **2014**, *4*, 1301743.